Comparison of Energy Update Models for Wireless Sensor Nodes with Supercapacitors

Aravind Kailas
Algorithms, Models, and Systems Solutions, LLC
Charlotte, NC, USA
aravind.kailas@almosyso.com

Davide Brunelli
University of Trento
Povo, Italy
davide.brunelli@unitn.it

Mary Ann Weitnauer
Georgia Institute of Technology
Atlanta, GA, USA
mary.ann.weitnauer@ece.gatech.edu

ABSTRACT

The key motivation for this work is the fact that modeling energy storage devices such as supercapacitors (SCs) for wireless sensor networks (WSNs) is important for the design and performance assessment of harvesting-aware routing protocols of the future. In this paper, we present a circuit-based model (CBM), a good fit to the empirical data available in the existing literature, and compare it with a linear energy model (LEM) that is often used in literature. Simple closed-form expressions for the number of packets routed by a single node have been derived, and the main point was to point out that the modeling the energy storage medium, namely the SC, impacts the parameter of interest. Our modeling approach and the subsequent comparisons show that the choice of models implies a significant difference in the throughput per node.

Categories and Subject Descriptors

C.4 [**Performance of Systems**]: Modeling techniques; I.6.4 [**Simulation and Modeling**]: Model Validation and Analysis; I.6.5 [**Simulation and Modeling**]: Model Development—*modeling methodologies*; J.2 [**Computer Applications**]: Physical Sciences and Engineering—*electronics*

Keywords

Embedded systems, harvesting, leakage, supercapacitors, wireless sensor networks

1. INTRODUCTION

The network lifetime of energy-harvesting embedded systems that store their energies on rechargeable batteries (RBs) will be defined by the finite cycle life defined as the number of charge and discharge cycles before they fail to hold a charge [5]. Another type of storage medium, the supercapcitor (SC), offers an attractive alternative. SCs do not hold as much energy as the RBs, but can be discharged and recharged on the order of a million times [2]. This paper models an SC, and hence the energy dynamics in an SC that will subsequently aid in the network simulation and analysis of such future systems.

Permission to make digital or hard copies of all or part of this work for personal or classroom use is granted without fee provided that copies are not made or distributed for profit or commercial advantage and that copies bear this notice and the full citation on the first page. Copyrights for components of this work owned by others than ACM must be honored. Abstracting with credit is permitted. To copy otherwise, or republish, to post on servers or to redistribute to lists, requires prior specific permission and/or a fee. Request permissions from Permissions@acm.org. *ENSSys'13,* November 13 2013, Roma, Italy Copyright 2013 ACM 978-1-4503-2432-8/13/11. . .$15.00. http://dx.doi.org/10.1145/2534208.2534223

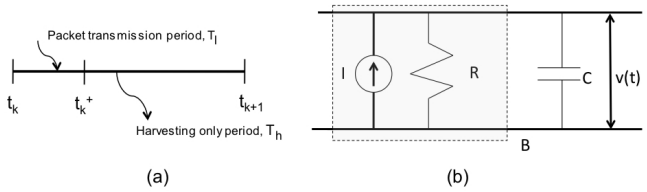

Figure 1: (a) A time slot, (b) generic circuit model for the SC.

Network performance evaluations when the SC is one of the (or the only) storage media on a sensor node have all assumed that the harvested energy and the energy cost of relaying a packet are each proportional to the time in the particular state of harvesting or relaying, respectively [8], [3]. This energy model is referred to as the linear energy model (LEM). However, recent empirical characterizations of SC charging circuits do not quite agree with the LEM and indicate that the charging circuit is significantly more complicated than just a direct connection between an energy harvester and a SC [7]. When connected directly to an energy harvester, the SC pulls the voltage across the harvester to a value that is usually very far from the optimal operating point, thereby increasing the charging time of the SC due to the impedance mismatch [2]. In this paper, we propose a circuit-based model (CBM) for the SC in which the voltage across the SC is computed assuming that the SC is in a simple resistor-capacitor circuit with a constant current source during the chafing and discharging modes. The current sources and resistances are different for each mode. In the paper, the proposed model is shown to be a better fit to the empirical data of [7]–[6]. The paper concludes with a simulation-based comparison of the two energy models and underscores the difference in the number of packets relayed by a single node when using the two models.

2. CIRCUIT-BASED MODEL

2.1 System Models and Assumptions

The SC is assumed to leak and harvest energy continually. Packets are assumed to be equal-length and transmitted periodically at a rate of $\frac{1}{T_\ell + T_h}$. If the routing algorithm selects the node, the node relays the packet as shown in Fig. 1. The period of activity comprising route selection and relay-

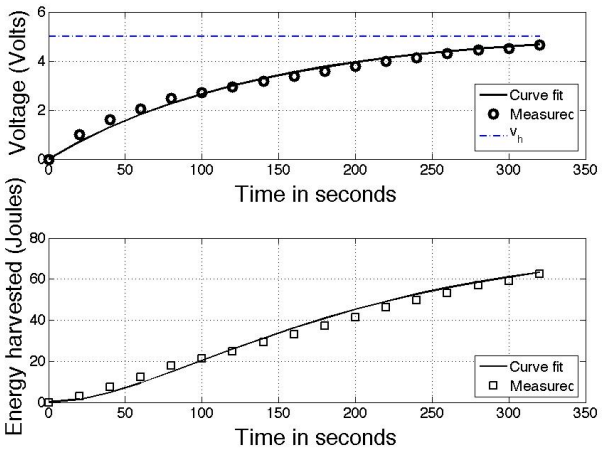

Figure 2: Pulse frequency modulated (PFM) charging of two 10 F SCs in series [7].

ing of the packet is assumed to be T_l seconds long. We define $t_k^+ = t_k + T_l$, where t_k defines the beginning of the k-th time slot. The remainder of the time slot until the arrival of the next packet is T_h seconds long. It follows that $t_{k+1} = t_k^+ + T_h$.

Our circuit-based model (CBM) is composed of the SC with Farad value C, and voltage $v(t)$, and the rest of the circuit is represented by its Norton Equivalent, which includes a constant current source, with current I and a parallel resistance, R. This circuit is modeled by a first order differential equation, and the solution or the voltage across the SC at any time t is given by:

$$v(t) = v(0^+)e^{\frac{-t}{\tau}} + IR(1 - e^{\frac{-t}{\tau}}),$$

where $\tau = RC$. We use plots from [5] and [7] to define I and R for each of the two modes: Charging and Discharging. Subsequently, we validate them using our own experiments.

2.2 Charging Model for the Supercapacitor

In this mode, I and R in the above equation are replaced by source current, I_h, and the equivalent charging resistance, R_h. The energy harvester setup that is used to extract R_h is similar to the pulse frequency modulated (PFM) charging circuit used in [7]. By exploiting a buck configuration controlled to track the maximum power point of the photovoltaic cell, the energy harvester setup behaves like a voltage regulator in which the current delivered is dependent on the current provided by the solar cell. In the experiment, a single 4.7 F SC with a maximum operating voltage of 5.5 V is used; voltages are bounded between 0 V and 5 V, implying that $v(0^+) = 0$.

Fig. 2 shows the voltage across two 10 F SCs in series (an equivalent capacitance of 5F SC) when charged at constant current in harvesting mode. In this mode, I and R in the above equation are replaced by I_h and R_h. We denote the product $I_h R_h$ by v_h. Since in Fig. 2, $v(0^+) = 0$, the values of the source current I_h and the equivalent resistance, R_h, for this RC charging circuit are obtained by fitting the second term of the above equation to the 'measured points' in Fig. 2. This yields $R_h = 27.56\ \Omega$, $I_h = 0.178A$ and $\tau_h = 140s$. While the solution of the differential equation during the time $T_h : t_k^+ \rightarrow t_{k+1}$, when the SC voltage is given by $v(t_{k+1}) = v(t_k^+)\alpha_h + v_h(1-\alpha_h)$, where $\alpha_h = e^{\frac{-T_h}{\tau_h}}$, and $\tau_h = R_h C$.

2.3 Discharging Model for the Supercapacitor

Our initial approach is to let the constant current "source" in Fig. 1 (b) represent the load current I_ℓ [9] and let the resistance R represent the SC leakage R_ℓ. We base our discharge model on Fig. 3 [5], which is a plot of leakage power, P_{Leakage}, vs residual energy, E_{Residual}, for a single 4.7 F SC. Our approach is to approximate the curve in this plot with a straight line, which we will show below is equivalent to modeling leakage power as the power dissipated through a resistor in parallel with an ideal capacitor. The leakage power is the power dissipated in R_ℓ. We may express E_{Residual} and P_{Leakage} as $E_{\text{Residual}} = \frac{Cv(t)^2}{2}$ and $P_{\text{Leakage}} = \frac{v(t)^2}{R_\ell}$. Combining these expressions gives the linear equation $E_{\text{Residual}} = \frac{R_\ell C P_{\text{Leakage}}}{2}$. To decide where on the plot to fit the line, we consider the minimum and maximum operating voltages of the SCs in [5]. The minimum and maximum energies of SCs 2.35 J and 7.61 J, respectively, thus we set the slope equal to $\frac{R_\ell C}{2}$ yields $R_\ell = 4478\ \Omega$. Because the energy harvesting and radio circuits are independent, the solution of the differential equation during the time $T_\ell : t_k \rightarrow t_k^+$ is given by: $v(t_k^+) = v(t_k)\alpha_\ell + v_\ell(1-\alpha_\ell)$, where $v_\ell = -|I_\ell - I_h|\,(R_\ell \parallel R_h)$, $\alpha_\ell = e^{\frac{-T_\ell}{\tau_\ell}}$, and $\tau_\ell = (R_\ell \parallel R_h)C$.

2.4 Obtaining R_h and R_ℓ Experimentally

Because the values of the equivalent charging and discharging resistances, R_h and R_ℓ, respectively, depend on the technology of the manufacturer thus different SCs from different manufacturers can feature slightly different R_h and R_ℓ. So, we conducted experiments under conditions similar to references [5] and [7] on a single 4.7 F SC to extract our parameters for the RC circuits during the two modes. We used the SC from Cooper Bussman [1]. Usually SCs have a limited maximum voltage (2.5 V or 5.5 V as in our case). The solar cell used was a 178 × 166 mm Polycrystalline Photovoltaic module with 7.6 V as nominal voltage and 280 mA as nominal current. The maximum power point tracking (MPPT) converter featured a step down, and provided a suitable output voltage to charge the SC. Of course in our experiments, the light intensity was much less. The intensity was regulated during our experiments to ensure constant currents. Using our experiments, we were able to obtain $R_h = 28\ \Omega$, $I_h = 0.18A$ and $\tau_h = 140s$. To extract the SC leakage resistance, R_ℓ, a maximum current consumption of a 100 mA is considered for a single 4.7 F SC. Following the curve approximation approach similar to that described in 2.3, setting the slope equal to $\frac{R_\ell C}{2}$ yields $R_\ell = 4478.1\ \Omega$. It is remarked that the values of R_ℓ and R_h extracted using our experiments on a 4.7 F SC are very close (second decimal place) to what would be extracted from [5] and [7], respectively, using similar fitting techniques.

2.5 Energy Update Equations for the Circuit-Based Model

The joint-voltage update equation for the time period $t_k \rightarrow t_{k+1}$ can be written as $v(t_{k+1}) = \beta_{hl} v(t_k) + \xi_{hl}$, where $\beta_{hl} = \alpha_h \alpha_\ell \approx 1$ and $\xi_{hl} \approx v_h(1-\alpha_h)$. Noting $E(t_{k+1}) = \frac{1}{2}C[v(t_{k+1})]^2$ and squaring both sides of the joint-voltage update equation, we write the energy update equation for $t_k \rightarrow t_{k+1}$ as $E(t_{k+1}) = \beta_{hl}^2 E(t_k) + C\xi_{hl}\alpha_h v(t_k) + \frac{1}{2}C\xi_{hl}^2$. It can be observed that in the above equation, the 2-nd term depends on the voltage. This means that the energy is a *nonlinear* update equation.

3. LINEAR ENERGY MODEL

In this section, the energy harvesting and leakage in a SC is modeled using what we refer to as an linear energy model (LEM). Following the same notations from the previous sections, for the time duration $t_k \rightarrow t_{k+1}$, the energy update equation is given by $E(t_{k+1}) = \alpha_\ell^2 E(t_k) - E_{\text{load}} + E_{\text{harvested}}$, where E_{load} is the energy consumed in routing a packet and $\alpha_\ell = e^{\frac{-T_\ell}{\tau_\ell}} = 1 - (8.9e^{-6}) \approx 1$ for 50% duty cycle, $\alpha_\ell^2 E(t_k) \approx E(t_k)$, and $E_{\text{harvested}} = \gamma(T_\ell + T_h)$ is the energy harvested with a rate of harvesting γ. One of the main differences between the CBM and LEM is that E_{load} is "independent" of the voltage (or energy) across the SC, and is fixed. So, our choice of E_{load} will determine the time range when the two energy models will have the same slope of residual energy versus time. In this letter, we choose E_{load} such that the slopes are equal at the start, when the SC is fully charged. From the energy update equation, it can be observed that the LEM is "decoupled" in the sense that the energy harvested and the energy consumed in routing a packet (the load energy) are simply added in the energy update equations. This approach is consistent with the "linear energy versus time" leakage models that have been assumed in the existing literature, exemplified by [4] and its references.

In a real system, the capacitor's voltage will change dynamically. In order to power the sensed nodes, a DC/DC converter will be used to convert the capacitor's voltage to a constant voltage. In other words, if a DC/DC converter is used, its efficiency changes accordingly to the input voltage and to the current absorbed by the load. Anyway we consider that a well performing DC/DC converter has a wide and flat efficiency for a wide range of the input voltage and the current drawn from the load is usually below 30 mA. It is an order of magnitude lower than the maximum current and DC/DC converter usually can provide (e.g., 500 mA). Thus, the output current variations have a negligible impact on E_{load}. Finally, it is remarked that there are also sensor nodes powered without DC/DC converter and with SCs as storage devices. These nodes just exploit the wide voltage supply range of the digital devices. For example a MSP430 micro controller (usually present in wireless sensor network nodes) can work with unregulated voltage from 1.8 V to 3.6 V, which is a pretty wide range where our model can be used without additional issues.

4. COMPARING THE TWO ENERGY UPDATE MODELS

One of the goals of this whole analysis has been to model the charging-discharging in a SC accurately, and to determine

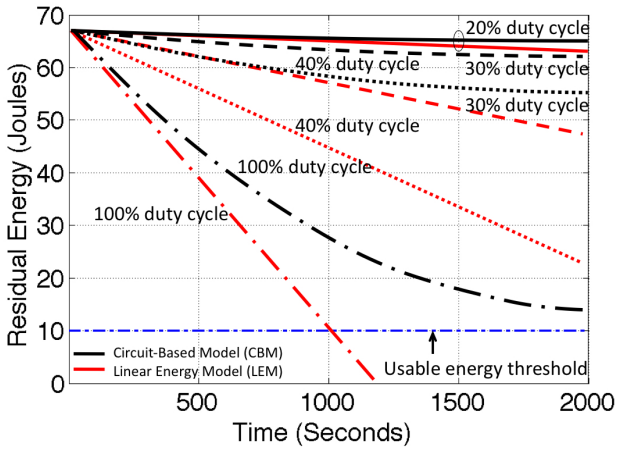

Figure 3: The residual energy versus time for the packet rate = 1.

the maximum number of packets sustained by a SC before its voltage drops, resulting in the SC energy falling below a threshold (i.e., minimum energy to route a packet), which would render the SC temporarily unusable. The duty cycle is defined as the ratio $\frac{T_\ell}{T_h+T_\ell}$. Both CBM and LEM model the leakage of the SC the same way, through the coefficient on the term $E(t_k)$ term, which makes leakage a function of the voltage drop across the SC. One difference between the LEM and CBM models is that in LEM, the harvesting and loading effects are respectively modeled by two additive constants in the update equation, while in CBM, there is only one constant term, which strictly depends on both harvesting and loading factors (v_h, v_ℓ, α_h, and α_ℓ). However, the most important difference is that CBM has a voltage-dependent term strictly depends on all of the same four factors as the constant term; this implies that also the voltage term cannot be said to be just the "harvesting" term or just the "loading" term.

Simulations of residual energy also show significant differences between the two models. Fig. 3 is a plot of the residual energy on the SC for a single node versus time using the two energy models described above for different duty cycles, and the packet rate is chosen to be 1. In Fig. 3, duty cycles of 20%, 30%, 40% (adaptive scenarios for applications as in [6]), and 100%. Firstly, it can be seen that at any time, the residual energy on the SC increases as the duty cycle decreases. It is noted that high duty cycles correspond to high values of T_ℓ, implying more energy consumption due to longer packets. The red lines (or the linear-like curves [1]) denote the variation in the residual energy with time using the LEM, and the black curves denote the same using the CBM. The blue (or horizontal) dash-dot line indicates the "unusable energy hysteresis," or usable energy threshold, which renders the SC useless if the voltage drops below this value [5]. With increasing time, the residual energy computed using the linear energy model is always less than the energy computed using the more accurate CBM. As stated, this difference is because in the latter model, the load and the

[1]The curves are not strictly linear because the α^2 coefficient is not exactly equal to one.

harvested energies are modeled as a function of the voltage drop across the SC at any time. Moreover, this difference becomes stark as the "harvesting only" period decreases.

5. MAXIMUM NUMBER OF PACKETS ROUTED BY THE SUPERCAPACITOR

In this section, we determine the number of packets that can be relayed by a node, when it is one of the p nodes in a cluster. An expression for the maximum number of bits that can be routed by a node before it's rendered unusable and needs recharging, i.e., when the voltage across the SC-parallel combination drops below a certain threshold $\mathcal{T}$ can be derived with the assumption that a node routes a packet once every p time slots. To determine the bottleneck of the proposed empirical model of the SC, the number of nodes in the network was chosen to be the parameter that would determine how frequently every node would transmit a packet, all packets being equally important.

5.1 Circuit-Based Model

Without loss of generality, we assume that the node transmits a packet during the first time slot, or $v_1 = I_h R_h = \sqrt{\frac{2E_{\max}}{C}}$. So, $v_{p+1} = v_1\hat{\beta} + \Delta V_p$, where $\hat{\beta} = \alpha_\ell \cdot \hat{\alpha}_h$, $\Delta V = v_h(1-\hat{\alpha}_h)+v_\ell(1-\alpha_\ell)\hat{\alpha}_h$, and $\hat{\alpha}_h = \exp\left\{\frac{-[T_h+(p-1)(T_\ell+T_h)]}{\tau_h}\right\}$. After the node has routed $n-1$ packets, i.e, at $k=(n-1)p+1$, we have $v_k = v_1\hat{\beta}^n + \left(\sum_{i=0}^{n-1}\hat{\beta}^i\right)\Delta V_p$. Let us also assume that after routing the n-th packet, the voltage across the SC-parallel combination drops below $\mathcal{T}$. Setting $v_k = \mathcal{T}$, we have $\mathcal{T}v_1\hat{\beta}^n + \underbrace{\left(\sum_{i=0}^{n-1}\hat{\beta}^i\right)}_{=\frac{1-\hat{\beta}^n}{1-\hat{\beta}}}\Delta V_p$, yielding

$$n = \log\left\{\frac{\mathcal{T}(1-\hat{\beta})-\Delta V_p}{v_1(1-\hat{\beta})-\Delta V_p}\right\}(\log\hat{\beta})^{-1},$$

the maximum number of packets routed by the SC, and $(n-1)p+1$ is the maximum number of time slots for which the SC was 'useful.'

5.2 Linear Energy Model

Next, the maximum number of bits that can be routed by a single relay using a SC using the LEM is derived. $E_1 = \alpha_1 E_{\max} - E_{\text{load}} + \gamma_1$, where $\alpha_1 = \alpha_\ell^2$, and $\gamma_1 = \gamma T_h$, where γ is the energy harvested per unit time. If there are p nodes in the network, then every node routes a packet every $\frac{1}{p}$-th of the time. So, $E_2 = \alpha_2 E_1 + \gamma_2 = \alpha_1\alpha_2 E_{\max} - \alpha_2 E_{\text{load}} + \alpha_2\gamma_1 + \gamma_2$, where $\hat{\alpha}_\ell = e^{\frac{-(T_\ell+T_h)}{\tau_\ell}}$, $\alpha_2 = \hat{\alpha}_\ell^2$, and $\gamma_2 = \gamma(T_h+T_\ell)$. Now the first node routes a packet after p time slots.

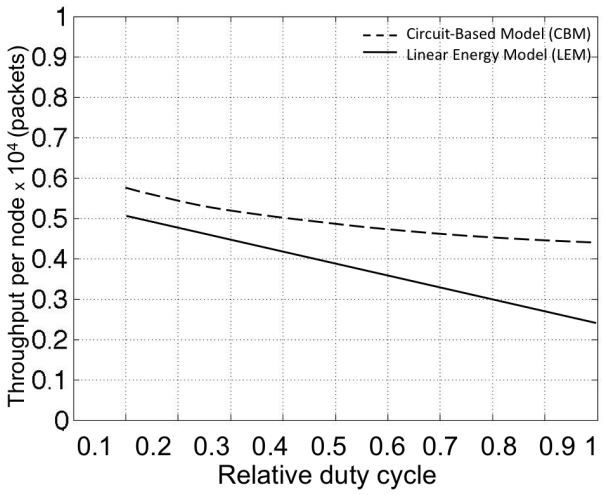

Figure 4: The number of packets routed per node per second versus relative duty cycle, $\frac{T_\ell}{T_h+T_\ell}$ for $p=1$ using CBM and LEM.

$$\begin{aligned}E_{p+1} &= \underbrace{\alpha_1^2\alpha_2^{p-1}}_{=:A}E_{\max} - \underbrace{\left(\sum_{i=0}^{1}\alpha_1^i\alpha_2^{i(p-1)}\right)}_{=:B}E_{\text{load}} \\ &\quad + \underbrace{\left(\sum_{i=0}^{1}\alpha_1^i\alpha_2^{i(p-1)}\right)\gamma_1 + \alpha_1\left(\sum_{i=0}^{p-2}\alpha_2^i\right)\gamma_2}_{=:E_{\text{harvested}}}, \\ &= AE_{\max} - BE_{\text{load}} + E_{\text{harvested}}.\end{aligned}$$

From above, it can be seen that the energy harvested and the energy consumed in routing a packet (the load energy) are decoupled from the energy lost due to the SC in the energy update equations. For $E_{k'}$ at any $k' = (m-1)p+a,\ a \in [0, p-1]$:

$$\begin{aligned}E_{k'} = \Bigg[&\alpha_1^m\alpha_2^{(m-1)(p-1)}E_{\max} - \left(\sum_{i=0}^{m-1}\alpha_1^i\alpha_2^{i(p-1)}\right)E_{\text{load}} \\ &+ \left(\sum_{i=0}^{m-1}\alpha_1^i\alpha_2^{i(p-1)}\right)\gamma_1 + \left(\sum_{i=1}^{m}\alpha_1^i\alpha_2^{(i-1)(p-1)}\right) \\ &\left(\sum_{i=0}^{p-2}\alpha_2^i\right)\gamma_2\Bigg]\alpha_2^{(a-1)} + \sum_{i=0}^{a-2}\alpha_2^i\gamma_2.\end{aligned}$$

Assuming that the residual energy stored in the SC-parallel combination drops below $\mathcal{T}'$ after routing the m-th packet, i.e., $a=1$, setting $E_{k'} = \mathcal{T}'$, and simplifying yields (1).

Fig. 4 is a plot of the number of packets routed per node versus duty cycle, $\frac{T_\ell}{T_h+T_\ell}$ for a single relay node network. The solid and dash-dot lines correspond to the throughputs using the LEM and the CBM, respectively. Using both models, the number of packets routed per node decreased with increase in the duty cycles. While this decrease is exponential for the CBM, it is linear for the LEM. It can be observed that the choice of models implies a significant difference in

$$m = \log\left\{ \frac{\mathcal{T}'\big(1-\alpha_1\alpha_2^{(p-1)}\big) + E_{\text{load}} - \gamma_1 - \alpha_2^{-(p-1)}\alpha_1\alpha_2^{(p-1)}\big(\sum_{i=0}^{p-2}\alpha_2^i\big)\gamma_2}{\alpha_2^{-(p-1)}E_{\max}\big(1-\alpha_1\alpha_2^{(p-1)}\big) + E_{\text{load}} - \gamma_1 - \alpha_2^{-(p-1)}\big(\sum_{i=0}^{p-2}\alpha_2^i\big)\gamma_2} \right\}\left\{ \log[\alpha_1\alpha_2^{(p-1)}] \right\}^{-1}. \quad (1)$$

number of packets relayed by a single node. Even when there is continual packet transmission, i.e., $\frac{T_\ell}{T_h+T_\ell} = 1$, there is a difference of more than 1000 packets routed using the two recursive energy models. The throughput differences between CBM and LEM at low duty cycles is simply because of the difference in the way the voltage (and hence the energy) is updated.

6. REMARKS ON THE MODELING ASSUMPTIONS

In order to enhance the contribution of our analysis and simulation, we connect the simulation parameters with some actual device statistics, such as the energy spent by a typical commercially available sensor mote or the energy gained by a harvesting platform that can be purchased. The big part of the power consumed by a 2.4 GHz sensor mote is spent mainly by activity of the radio. However, very rarely, specific sensing applications (e.g., wireless gas sensor nodes, video sensor networks, etc.) consume more energy. Generally a sensor mote needs about 20/30 mA to transmit and receive packets, which results in a power consumption during radio communication of about 50/80 mW if powered with rechargeable batteries. While, during the deepest sleep mode, the power consumed by such kind of sensor node can be very low, generally, 20 μA can be achieved without any particular low-power design. Using a more advanced architecture, the current consumption can be pushed closer to 2 μA during the deep sleep mode. Thus, the energy spent during a long interval (i.e., a day, a month, a year) depends mainly on the ratio between of the duration of active mode (i.e., with the CPU "ON" with or without radio "ON") and the interval where the node is put in deep sleep mode (i.e., the whole node in sleep).

On the other side, the energy generated by an energy harvester depends mainly on the exploited environmental source and on the size of the harvester. It is reasonable to have an harvester of the same size of the mote, thus a photovoltaic harvester can generate up to 30 mW under sunshine and about 2–3 mW in cloudy days or indoor. Micro wind turbines with diameters spanning a few cm will provide about 10 mW with 11 kph wind speed. Other environmental sources generate much less. For example, it is usually not possible to get no more than 3–4 mW from vibrations using a small-size piezoelectric harvester.

In practice, the MPPT circuitry simply manages the solar cell to obtain the maximum efficiency during the energy conversion. The whole harvester (solar cell+ MPPT) is suitable for the CBM model. When CBM is compared to other models available in the existing literature, usually, it is not possible to extract much information from the latter about the used conversion circuit (i.e., it is unknown whether a direct connection, an MPPT, or a simple DC/DC converter was used). So, the LEM considered in the paper is a basic implementation of photovoltaic harvester (i.e., direct connection), which also happens to be the most used model (e.g., a commercial solar charger).

Under constant environmental conditions (i.e., solar irradiance and temperature of the cell) the current provided by the cell is constant. This is a well- known relation of photovoltaic cells. However, if the environmental conditions change the output current (i.e., harvesting current, I_h) varies accordingly. Anyway, it is not dependent on the circuits state, thus, in our model, we considered constant ambient condition.

Regarding the constant-current load, I_ℓ, we remark that we have considered the worst-case scenario (i.e., the maximum load current for the whole T_ℓ). This enables to keep the model simple, while providing a comparison of the two models namely LEM and CBM. An extension of the proposed model that takes into account also a variable current load can be developed at the expense of increased complexity that would be greater than the improvements in accuracy. It is proposed to address this as a future work

Since the SC's voltage will drop over time, the sensor nodes are normally using DC/DC converters to convert the SC's voltage to the operational voltage of the sensor nodes. DC/DC converter efficiency is generally very high ($> 85\%$) and it depends mainly by the input voltage and the output current. In our model, the efficiency of the DC/DC converter can be included in the rate of the harvesting, γ_ℓ. Energy harvesters usually exploit boost, buck or boost-buck converters to convert voltage from the environmental transducers (e.g., photovoltaic cell, piezoelectric beam, etc.) to the desired output voltage supply. These DC/DC configurations are designed with very high efficiency over a wide range of operating conditions. We considered a worst case in our model by assigning a fixed efficiency and assuming the whole harvester to deliver 96% average efficiency.

On a summarizing note, we addressed the energy update model in a single node considered as a single system (energy harvester + energy storage + variable load) both during recharging and discharging the energy reservoirs. The reason is because all these parts are necessary to CBM and contribute to the final result. We remark that the harvester itself has a major contribution, and the way it is implemented is fundamental. In fact, the environmental energy collection can be made with a simple direct connection between the energy transducer (e.g., a solar cell) to the energy reservoir, and it is really inefficient, or by the adoption of specific circuits which maximize the conversion efficiency in any conditions. For this kind of harvesters, the LEM model is not a good fit. In a future work, it is planned to extend

the section of energy harvesting modeling and to propose a generalization usable for powering any embedded system of any size and not only a node of a WSN.

7. CONCLUSIONS

A novel, simple, analytical energy update model for SCs that is consistent with the available empirical data is presented in this paper. While it is true that a SC is not a normal capacitor, but it is not that different. The two key differences are the leakage and the charge distribution. We have already addressed leakage, while charge distribution is mainly a long-term effect, which appears only if SC is left in steady conditions for long intervals (i.e., no charging or discharging for hours). Compared to the more traditional energy models, the harvested and load energy terms in the proposed model are dependent on the voltage across the SC, and this significantly impacts the network analysis (e.g., throughput per node). In other words, the key difference between the CBM and the LEM is that the harvested and load terms in the energy update equations depend on the voltage across the SC in case of the CBM, but are constant for the case of the LEM. Extensions to this model such as accounting for a variable current load and module improvements for enhancing accuracy, and modeling energy harvesters using different environmental sources are some directions for future work.

8. REFERENCES

[1] Cooper bussman. `http://www.cooperindustries.com/content/public/en/bussmann/electronics/brands.html`, 2008. [Online; accessed 5-Sep.-2013].

[2] D. Dondi, A. Bertacchini, L. Larcher, P. Pavan, D. Brunelli, and L. Benini. A solar energy harvesting circuit for low power applications. In *Sustainable Energy Technologies, 2008. ICSET 2008. IEEE International Conference on*, pages 945–949, 2008.

[3] A. Kailas, M. A. Ingram, and Y. Zhang. A novel routing metric for environmentally-powered sensors with hybrid energy storage systems. In *Wireless Vitae*, pages 1–6, May 2009.

[4] L. Lin, N. Shroff, and R. Srikant. Asymptotically optimal power-aware routing for multihop wireless networks with renewable energy sources. *IEEE/ACM Trans. on Net*, October 2007.

[5] G. Merrett, A. Weddell, A. P. Lewis, N. Harris, B. Al-Hashimi, and N. White. An empirical energy model for supercapacitor powered wireless sensor nodes. In *17th International Conference on Computer Communications and Networks*, pages 1–6, Aug. 2008.

[6] C. Moser, L. Thiele, D. Brunelli, and L. Benini. Adaptive power management for environmentally powered systems. *IEEE Trans. Comput.*, 59(4), 2010.

[7] F. Simjee and P. H. Chou. Efficient charging of supercapacitors for extended lifetime of wireless sensor nodes. *IEEE Trans. Power Electron.*, 23(3):1526–1536, May 2008.

[8] T. A. Smith, J. P. Mars, and G. A. Turner. Using supercapacitors to improve battery performance. In *Power Electron. Specialists*, 2002.

[9] A. S. Weddell, N. R. Harris, and N. M. White. Alternative energy sources for sensor nodes: Rationalized design for long-term deployment. In *Instrumentation and Measurement Technology*, pages 1370–1375, May 2008.